

OPTIMIZATION OF TRIANGULAR FORMATION FLYING CONFIGURATIONS UNDER THE CIRCULAR AND ELLIPTIC THREE-BODY PROBLEM DYNAMICS MODELLING

Fabio Ferrari⁽¹⁾ and Michèle Lavagna⁽²⁾

⁽¹⁾⁽²⁾*Department of Aerospace Science and Technology, Politecnico di Milano, via La Masa 34, 20156 Milano, Italy, +39 02 23998365, [fabio1.ferrari;michelle.lavagna]@polimi.it*

Abstract: *The paper studies natural triangular formations of spacecraft under the Three-Body dynamics. An equilateral triangularly-shaped formation of spacecraft is assumed as a representative geometry to be studied. Initial configurations, which provide good performance in terms of formation keeping, have been investigated and key parameters, which mainly control the formation dynamics within the three-body system, have been identified. The evolution of spacecraft formation in the proximity of point periodic orbits about collinear libration points is studied. The analysis has been performed under several degrees of freedom to define the geometry, the orientation and the location of the triangle in the synodic rotating frame. The effect of different initial conditions sets on natural formation keeping performance is studied: the aim is to find optimal solutions in terms of initial condition sets which guarantee the maximization of performance factors, which have been introduced to evaluate formation keeping. The optimization is performed using a global optimization algorithm from the domain of soft computing, to exploit its great capability of investigating a large range of potential solutions in parallel, starting from not informed initial guess to maximize performance factors, whose mathematical expression is provided analytically.*

Keywords: *Formation Flying, Optimization, Genetic algorithm, Three-body problem, Relative dynamics.*

1. Introduction

Spacecraft Formation Flying in the proximity of libration points associated to a three-body system represents one of the most promising applications for space mission design. It provides the designer with the flexibility of having more than one flying platform to answer mission requirements and of exploiting the three-body trajectory design techniques to lower transfer and station keeping costs. Among others, observation, telecommunication and exploration missions can greatly benefit from this peculiar coupling. The design of classical spacecraft formations is usually characterized by a highly challenging trajectory and station keeping problem solving, to satisfy tight requirements on relative dynamics between each member of the formation. The exploitation of low acceleration regions such as the proximity of equilibrium points associated to a three-body system opens a new range of design opportunities, as three-body dynamics can be conveniently used to reduce such trajectory and station keeping needs.

Control strategies to maintain formations of spacecraft under three-body dynamics are being widely studied in the last decades, but very few studies of free relative motion between the spacecraft under this chaotic and unstable dynamics exist. Among them, Barden and Howell [1] exploited the natural motion on the center manifold near periodic orbits to reproduce tori of quasi-periodic trajectories that can be useful for the design of naturally bounded formations of spacecraft. Few

years later, Gómez et al. [2] derived regions around periodic orbits with zero relative velocity and radial acceleration, which ideally keep unchanged the relative distances between the spacecraft in the formation. Héritier and Howell [3] extended the analysis done by Gómez et al. and derived low drift regions (low relative velocity and acceleration) around periodic orbits, as quadric surfaces. Ferrari and Lavagna [4] generalized the work by Héritier and Howell to the whole three-body domain, identifying regions of zero relative acceleration and velocity (ZRAV loci) for large formations of spacecraft. Also, the relative dynamics of a three-spacecraft triangular formation have been investigated and suitable initial conditions have been found in the Earth-Moon system [4]. These studies focus on the analysis of the dynamics under the Circular Restricted Three-Body formulation. However, in general, natural three-body systems have orbits with non-zero eccentricities: the elliptic problem results then to be a better model to represent the real systems than the circular one. Controlled formations have been studied under the Elliptic Restricted Three-Body Problem (ER3BP) formulation [5] but still there is very little known about the free relative dynamics within this particular dynamical environment.

The present work aims to pursue previous studies on natural triangular formations of spacecraft under the Circular Restricted Three-Body Problem (CR3BP) [4] and under the more accurate model provided by the Elliptic Restricted Three-Body Problem (ER3BP) [6]. An equilateral triangularly-shaped formation of spacecraft is assumed as a representative geometry to be studied. One example of such a formation arrangement is the LISA mission [7], which consists of three identical spacecraft, placed around a reference point that orbits the Sun, following a circular path. Other examples of similar configurations are given by Cluster II [8] and Magnetospheric Multiscale Mission (MMS) [9] architectures: both of them employ a tetrahedral (triangular pyramid) formation to study Earth's magnetosphere.

The goal of the optimization process here implemented is to seek initial configurations of the triangular formation, which provide good performance in terms of formation keeping. The optimization is set up by considering all key parameters, which mainly control the formation dynamics within the three-body system, as variable of the problem. The evolution of spacecraft formation in the proximity of collinear libration point periodic orbits (Halo and Lyapunov orbits are considered) is studied and monitored. The analysis has been performed under several degrees of freedom to define the geometry, the orientation and the location of the triangle in the synodic rotating frame: one parameter defines the size of the triangle and five parameters describe unequivocally its location and orientation in the rotating frame. The relative velocity state between the spacecraft plays also an important role. The initial condition set includes all degrees of freedom considered in the analysis. Formation keeping performance is quantified by defining two performance indexes, to monitor shape and size changes of the triangular formation and to compare them against the desired dynamical behavior of the formation. This work aims to find optimal solutions in terms of initial condition sets which guarantee the maximization of performance factors. The optimization is performed using a global optimization algorithm from the domain of soft computing, to exploit its great capability of investigating a large range of potential solutions in parallel, starting from not informed initial guess to maximize performance factors, whose mathematical expression is provided analytically. This would provide enhanced tools to the mission designer, suitable to design the mission analysis of triangularly shaped formations in the proximity of libration points orbits, providing cost effective solutions in terms of formation keeping needs.

The paper is organized as follows. The background of three-body dynamics is initially recalled and the main features associated to the Circular and Elliptic Restricted Three-Body Problems are presented, highlighting peculiar solutions of interest for the case of study, such as families of periodic orbits. After having recalled three-body dynamics, the optimization problem is presented, including the description of the fitness function and the search space. Some results are then presented and discussed, before concluding remarks are summarized at the end of the paper.

2. Background: three-body dynamics

This section presents the dynamical models in use to describe the motion of the triangular formation. The dynamics of the spacecraft are described by using the Circular and Elliptic Restricted Three-Body Problem formulations. The equations of motion and the main features associated to these dynamical models are briefly recalled here.

2.1. Circular Restricted Three-Body Problem

The focus is on the motion of a small body (third body) that is attracted by two primaries, but it does not influence their motion. The two primaries are constrained to move on a circular orbit around their center of mass. It is common to express the equations of motion of the third body in a reference frame which is centered in the center of mass of the two primaries and rotates together with them (Figure 1).

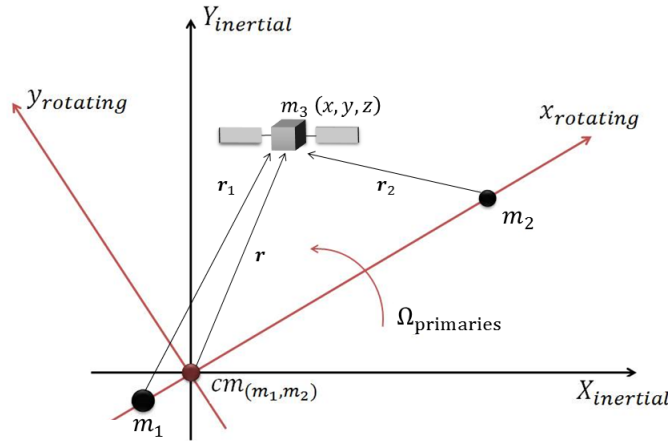


Figure 1. Rotating frame

The equations of motion are written in a nondimensional form, using the potential function associated to the problem

$$U = \frac{1}{2}(x^2 + y^2) + \frac{1 - \mu}{r_1} + \frac{\mu}{r_2} \quad (1)$$

with

$$r_1 = \sqrt{(x + \mu)^2 + y^2 + z^2} \quad (2a)$$

$$r_2 = \sqrt{(x - (1 - \mu))^2 + y^2 + z^2} \quad (2b)$$

The parameter μ is called mass ratio and it is defined as follows

$$\mu = \frac{m_2}{m_1 + m_2} \quad (3)$$

The equations of motion are written as

$$\begin{cases} \ddot{x} - 2\dot{y} = U_x \\ \ddot{y} + 2\dot{x} = U_y \\ \ddot{z} = U_z \end{cases} \quad (4)$$

where the notation $U_{(\cdot)}$ means partial derivative of the potential with respect to the variable (\cdot) .

2.2. Lyapunov and Halo families

Infinite possibilities, in terms of periodic orbits, are known to exist when considering the Circular Restricted Three-Body Problem.

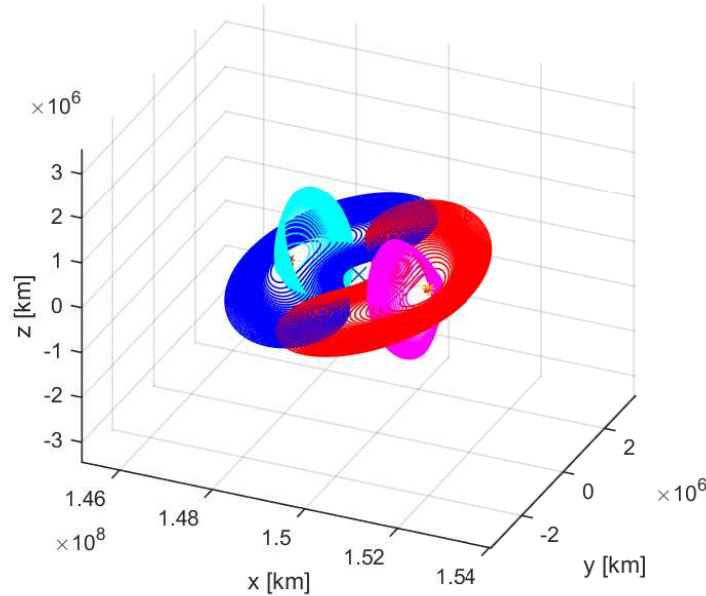


Figure 2. Lyapunov (planar) and Halo (3D) families about collinear libration points: blue and cyan are families about L1, red and magenta about L2 of Sun-Earth system

Periodic motion about libration points is used in this work to provide a reference trajectory to the formation. Among the many possibilities, reference orbits have been chosen among Lyapunov and Halo families about L1, L2 and L3. Figure 2 shows families of Lyapunov (planar) and Halo (three-dimensional) orbits about the first and second lagrangian point of Sun-Earth three-body system.

2.3. Elliptic Restricted Three-Body Problem

In the CR3BP the primaries are constrained to move on circular orbits: for real systems, it represents a simplification and in some cases it can lead to large errors in the description of the third body motion. The elliptic problem avoids the simplification of the circular case, considering the elliptical path of the primaries about their common center of mass, consistently with their two-body problem modeling.

In analogy to the circular problem, the equations of motion of the third body are expressed in the rotating reference frame. Unlike the CR3BP, the position of the primaries is not fixed in the rotating frame as they move along elliptical orbits: their relative distance ρ is not constant in time

$$\rho = \frac{p}{1 + e \cos f} \quad (5)$$

p is the semi-latus rectum, f is the true anomaly and e is the eccentricity of the primaries orbit. As a result, when seen from the rotating frame, the position of the primaries pulsates along the x axis. The equations of motion are then written in a rotating-pulsating reference frame.

The equations of motion are written in a nondimensional form [10], using the pseudo-potential function associated to the problem [11]

$$U = \frac{1}{1 + e \cos f} \left[\frac{1}{2}(x^2 + y^2 - z^2 e \cos f) + \frac{1 - \mu}{r_1} + \frac{\mu}{r_2} \right] \quad (6)$$

where r_1 and r_2 represent the distance of the particle from the primaries (m_1 and m_2), while μ is the mass ratio of the planetary system

$$\mu = \frac{m_2}{m_1 + m_2} \quad (7)$$

The equations of motion can be expressed as

$$\begin{cases} x'' - 2y' = U_x \\ y'' + 2x' = U_y \\ z'' = U_z \end{cases} \quad (8)$$

where $(\cdot)'$ and $(\cdot)''$ indicate first and second derivative with respect to the true anomaly, while the notation $U_{(\cdot)}$ indicates the partial derivative of the pseudo-potential with respect to the variable (\cdot) . The system (8) is non-autonomous, since the motion of the third body depends on the position of the primaries.

2.4. Periodic orbits in the ER3BP

The Circular Restricted Three-Body Problem is known to have infinite periodic solutions which can be collected into families of orbits with continuously varying period. When the problem is

generalized to the elliptic one, this is not valid anymore: the ER3BP admits only isolated periodic orbits, with well-determined periods. This is due to the fact that the motion of the particle depends explicitly on time, i.e. on the location of the primaries. Since the time-dependent terms in (8) are periodic with period 2π (one revolution of the primaries between their common center of mass), then periodic solutions of the ER3BP must be periodic of period $T = 2\pi N$, with $N = 1, 2, \dots$

In this work, periodic orbits in the ER3BP have been generated starting from orbits in the CR3BP with similar period, through eccentricity continuation techniques. Examples of how periodic orbits can be computed can be found in [12] and [13].

3. The optimization problem

The study is here presented: the criteria and assumptions driving the numerical set-up of the optimizer are shown in this section. As already mentioned, the work focuses on the study of the free dynamics of a formation of satellites, with the goal to find suitable initial configurations which allow for good performance in terms of formation keeping. In the following paragraphs, the meaning of “initial configuration” and “formation keeping performance” will be explained and clarified. Also, criteria driving the selection of suitable initial configurations will be defined and motivated.

As mentioned, the goal of the optimizer is to explore a very large domain of initial conditions and to find the optimal set in terms of maximization of formation keeping performance, quantified thanks to some performance factors. To this aim, the optimizer is chosen to implement a genetic algorithm.

The problem is formulated as follows. Three identical spacecraft are placed at the vertexes of an equilateral triangle. The triangular formation is located in the three-dimensional space and its dynamical state is initiated by selecting relative initial position and velocity between the spacecraft. The dynamics of the spacecraft are integrated forward and their relative positions are monitored in time.

The next paragraphs discuss the set up of the optimization problem, including the description of the initial population set, the boundaries of the search space domain and the fitness function.

3.1. Initial population set

The initial population set includes all parameters needed to initiate the numerical integration of the spacecraft dynamics. As mentioned, three identical spacecraft are located at the vertexes of an equilateral triangle. Several parameters are used to unequivocally define the initial geometry, location and orientation of the triangular formation, as well as the relative velocity of each spacecraft at the beginning of the numerical integration. More in detail, the geometry of the triangle is defined by the parameter d : it represents the initial size of the formation being it the distance between each spacecraft and the barycenter of the equilateral triangle. Figure 3 shows the triangular formation, where x , y and z are directed as the axes of the rotating frame. The relative orientation of the formation with respect to the rotating frame is specified by the three components of the normal to the triangle plane \mathbf{n} and by the angle θ which represents positive rotation about \mathbf{n} axis as shown in Figure 3.

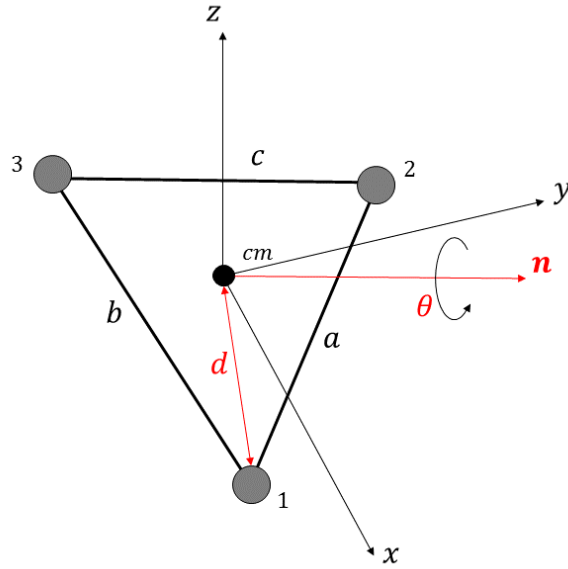


Figure 3. Triangular formation in the rotating frame

The location of the barycenter of the formation in the three-dimensional space is specified by selecting a reference orbit about one of the collinear lagrangian points. Finally, velocities of all spacecraft are chosen, to initiate consistently their dynamics. Summarizing, the initial population set includes the following parameters:

- d : distance between each spacecraft and the center of mass of the formation
- \mathbf{n} : normal to the triangle plane (three-component unity vector)
- θ : rotation about \mathbf{n} axis
- \mathbf{X}_{ref} : reference orbit (initial conditions)
- \mathbf{v}_1 : velocity vector of first spacecraft
- \mathbf{v}_2 : velocity vector of second spacecraft
- \mathbf{v}_3 : velocity vector of third spacecraft

Once the initial configuration has been selected, the equations of motion are integrated forward in time for each spacecraft as they evolve near the reference trajectory. The evolution of the formation is monitored using performance factors.

3.2. Search space domain

To set up the optimization process, the search space is clearly defined, by identifying boundaries the parameters are allowed to range within. The order of magnitude of the size of the formation d has been chosen by analogy with existing missions employing similar formation configurations: for example, the size of Cluster II [8] and MMS [9] formations varies from few kilometers up to few thousands of kilometers. In this work, a significantly wider range of variability is allowed for the initial size of the triangle that can range between 1 m and 10^5 km. No constraints are imposed on the relative orientation of the triangle, meaning that no limitations are imposed on \mathbf{n} and θ , except for the need of keeping \mathbf{n} as an unit norm vector. For what concerns the orbital path of the spacecraft,

the analysis has been performed by considering families of Lyapunov and Halo orbits about L1, L2 and L3 in the Sun-Earth three-body system. Each component of the initial velocity vector of each spacecraft is allowed to range within $\pm 20\%$ range with respect to the velocity on the reference orbit \mathbf{v}_{ref} . Table 1 summarizes the initial population set, highlighting the effect of the parameter on the initial configuration of the formation and its limiting range.

Table 1. Initial population set

Parameter	Range
d	1 m - 10^5 km
\mathbf{n}	not limited, with $\ \mathbf{n}\ = 1$
θ	0 - 2π
\mathbf{X}_{ref}	L1,L2,L3 Lyapunov and Halo families
\mathbf{v}_1	$\mathbf{v}_{\text{ref}} \pm 20\%$
\mathbf{v}_2	$\mathbf{v}_{\text{ref}} \pm 20\%$
\mathbf{v}_3	$\mathbf{v}_{\text{ref}} \pm 20\%$

3.3. Fitness function

After the initial population has been settled, the dynamics of the three spacecraft are integrated forward in time as they evolve near the reference orbit. The fitness function refers to the evaluation of formation keeping performance after one complete orbital period associated to the reference orbit.

The ideal formation keeping condition can be synthesized as no change in shape and size of the initial triangular configuration as it evolves along the reference orbit. This condition is of course impossible to obtain at each time instant, if the formation is free and uncontrolled, in an extremely chaotic and non-linear environment such as a three-body system. However, it is possible to seek preferred initial configurations which lead to small changes in shape and size of the formation during its evolution on the orbit, and then to cheaper formation keeping needs. In order to evaluate how the geometrical properties of the formation are maintained, the shape and the size of the triangle are monitored during the evolution of the three spacecraft along the orbit. It is here proposed a way to measure formation keeping performance, to quantify both shape and size changes. To this purpose, two performance factors are defined: the *Shape Factor* (SF), which takes into account for the change in the shape of the triangle, and the *Size or Dimension Factor* (DF), which takes into account for the change in size of the triangular formation. These performance indexes have been introduced by the authors in a previous work [4], where the interested reader can find more details about their mathematical definitions. The following paragraphs recall the analytical expressions of the two indexes.

3.3.1. Shape Factor

The Shape Factor (SF) is defined as

$$SF = e^{-\sqrt{(\ln \varepsilon_1)^2 + (\ln \varepsilon_2)^2}} \quad (9)$$

with

$$\varepsilon_1 = \frac{a}{b} \quad \varepsilon_2 = \frac{a}{c} \quad (10)$$

where a , b and c represent the current length of the sides of the triangle, with reference to Figure 3.

Note that the Shape Factor is a nondimensional variable that ranges from 0 to 1. It can be easily verified that the shape is unchanged if and only if

$$\varepsilon_1 = \varepsilon_2 = 1 \quad (11)$$

and then the ideal condition of unchanged shape is

$$SF = g(\varepsilon_1, \varepsilon_2) = g(1, 1) = 1 \quad (12)$$

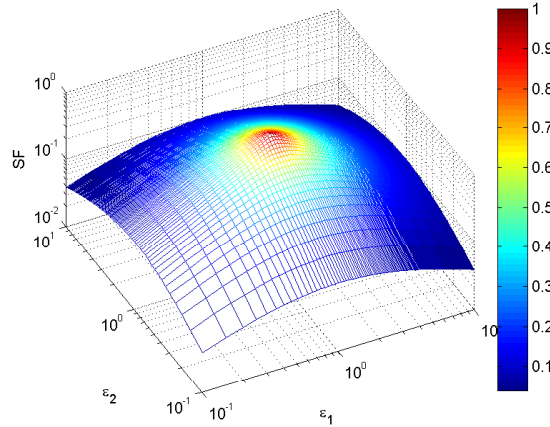


Figure 4. Shape Factor (logarithmic scale)

Figure 4 shows the 3D graphics of Equation (9), which represents the Shape Factor function.

3.3.2. Dimension Factor

The Size or Dimension Factor (DF) monitors the size of the triangle during the evolution of the formation and it is defined as

$$DF = \frac{\eta_1 + \eta_2 + \eta_3}{3} \quad (13)$$

with, referring to Figure 3

$$\eta_1 = \frac{a}{a_0} \quad \eta_2 = \frac{b}{b_0} \quad \eta_3 = \frac{c}{c_0} \quad (14)$$

Note that this index is also nondimensional but here the ratios are computed for each side, with respect to its initial length, denoted by subscript $_0$. The Dimension Factor equals one only at the initial time and when the average size of the formation is maintained. Differently from the Shape Factor, it needs information on the initial state of the formation and provides a measure of the size of the triangle at a certain time after initial time. Roughly speaking, $DF=10$ at $t = t_1$ (with $t_1 > t_0$) means that the triangle is, on average, 10 times bigger than its initial size at $t = t_0$.

3.3.3. Implementation

From the numerical point of view, the evaluation of the fitness function $f(x)$ includes the integration of the equations of motion of the circular or elliptic problem for all three spacecraft and the evaluation of SF and DF after one period of the reference orbit. The optimal condition is represented by no change in shape and size of the formation, which is given by

$$\begin{aligned} SF &= 1 \\ DF &= 1 \end{aligned}$$

The ultimate figure, to be minimized by the optimizer is written as

$$f(x) = (1 - SF(x)) + |1 - DF(x)| \quad (15)$$

where x indicates the initial population set and both SF and DF are computed after the numerical integration on the dynamics. Equation 15 is equal to zero if $SF = DF = 1$, meaning that its minimum corresponds to the optimal initial condition set in terms of formation keeping performance. More in detail, Eq. 15 can be written as

$$f(x) = (1 - (e^{-\sqrt{(\ln \frac{a}{b})^2 + (\ln \frac{a}{c})^2}})) + |1 - \frac{a}{a_0} + \frac{b}{b_0} + \frac{c}{c_0}| \quad (16)$$

where the effects of initial conditions (a_0, b_0, c_0) and of the outcome of the integration of the dynamics (a, b, c) is clearly highlighted.

4. Results

This section presents the results of the optimization process. The optimal initial configurations, limited to the domain of parameters defined in the previous section, have been found. The first part is dedicated to results obtained under the Circular Restricted Three-Body Problem formulation, while the last part of this chapter shows some results referred to the elliptical case.

Table 2 summarizes the results of the optimization, grouped according to the family of reference orbit. The results shows that the optimization does not converge to a good solution for the case of L1 orbits, whereas suitable solutions are found concerning L2 and L3 orbits. The overall best case is found for Halo and Lyapunov orbits about L3.

As mentioned, the optimizer does not converge to good initial set in terms of formation keeping performance for the case of L1 orbits. However, the initial orientation of the L1 solutions is found in agreement with results obtained through Monte Carlo simulations [4]. More in detail, the triangle lies initially on the y,z plane as shown in Fig. 5(a) (solution for lyapunov family) and in Fig. 5(b) (for halo family).

Regarding L2 solutions, the optimizer is shown to converge to good results, in particular for the case of lyapunov orbits. Figure 6 shows that the geometry of the formation is preserved after one orbital period (indeed SF=1.00, DF=1.07) while its orientation changes with respect to its initial configuration.

Table 2. Results of the optimization

Reference orbit	SF	DF
Lyapunov L1	2e-3	59
Halo L1	4e-3	24
Lyapunov L2	1.00	1.07
Halo L2	0.75	1.00
Lyapunov L3	1.00	1.00
Halo L3	1.00	1.00
Halo L3 (ER3BP)	1.00	1.00

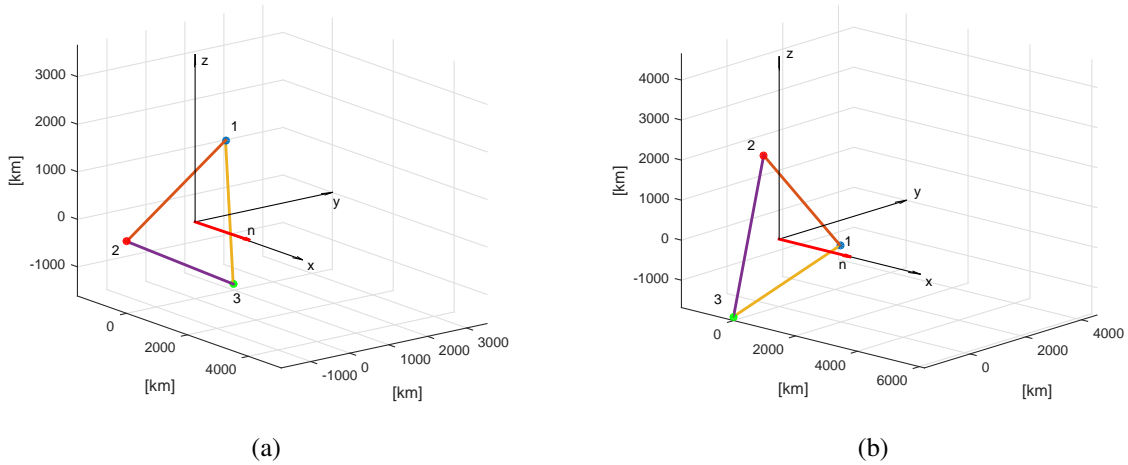


Figure 5. Optimal relative orientation for L1 (a) lyapunov and (b) halo families of orbits

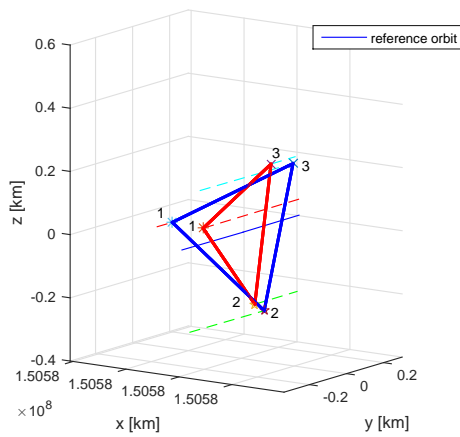


Figure 6. Triangular formation at time t_0 (red) and after one orbital period (blue) (L2 lyap)

The best solutions are found when considering orbits about L3. In this case the geometry and orientation of the formation is fully preserved after one orbital period, as shown in Fig. 7, where the formation at t_0 is exactly overwritten by the formation after one orbital period. The three spacecraft are located on nearly periodic orbits nearby the reference halo orbit, since their motion is periodic with nearly the same period of the reference orbit.

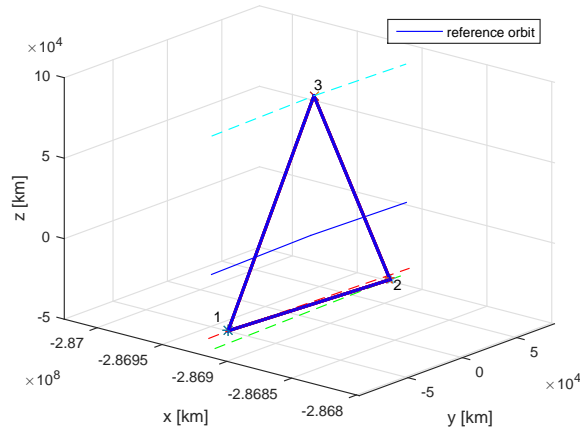


Figure 7. Triangular formation at time t_0 (red) and after one orbital period (blue) (L3 halo)

Figure 8 shows an example of how performance factors behave in time during the evolution of the formation on the reference orbit. The abscissa represents nondimensional time, normalized to one period of the reference orbit (in this case the time span goes from 0 to one period T_{orb}). As mentioned, the fitness function includes the evaluation of formation keeping performance at $t = T_{orb}$. SF and DF functions exhibit a periodic behavior: in both cases the performance reaches a minimum after half orbit and it increases towards the optimal condition at the end of the orbital period. This means that the geometry of the formation is not kept constantly as it evolves along its orbit, but it reaches the optimum periodically, with a period equal to the period of the reference orbit.

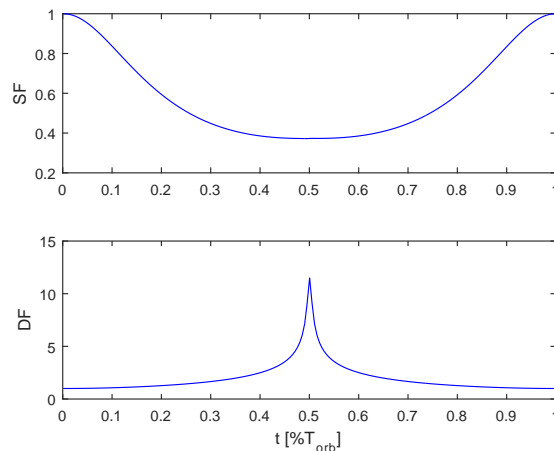


Figure 8. Time evolution of performance factors (L3 halo)

In the case of Lyapunov family about L3 the optimizer converges to a small orbit, and the formation has a characteristic size comparable to the amplitude of the orbit. Figure 9 shows the evolution of the triangular formation during one orbit and Fig. 10 shows the behavior in time of performance factors. In this case the formation deforms on the orbit, with lowest formation keeping performance at $1/4 T_{ref}$ and $3/4 T_{ref}$. At that point, the triangle collapses nearly onto a line but it naturally gets back to its initial geometrical configuration after $T_{ref}/2$ from t_0 .

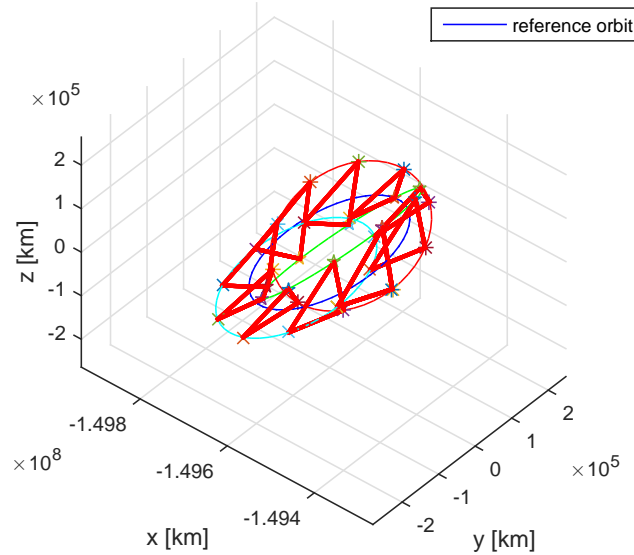


Figure 9. Time evolution of the triangular formation (L3 lyap)

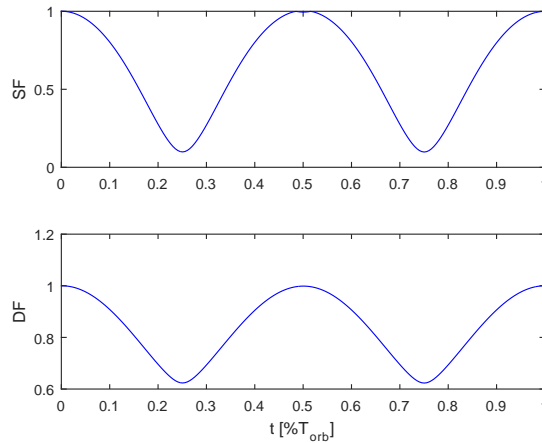


Figure 10. Time evolution of performance factors (L3 lyap)

It is worth to notice that the three spacecraft experience periodic motion and their paths are actually out-of-plane orbits in the proximity of the reference Lyapunov orbit (Fig. 11).

The optimal initial configuration, in case of L3 halo and Lyapunov orbits are shown in Fig. 12(a) and in Fig. 12(b). In terms of relative orientation, these configurations are in agreement with the results

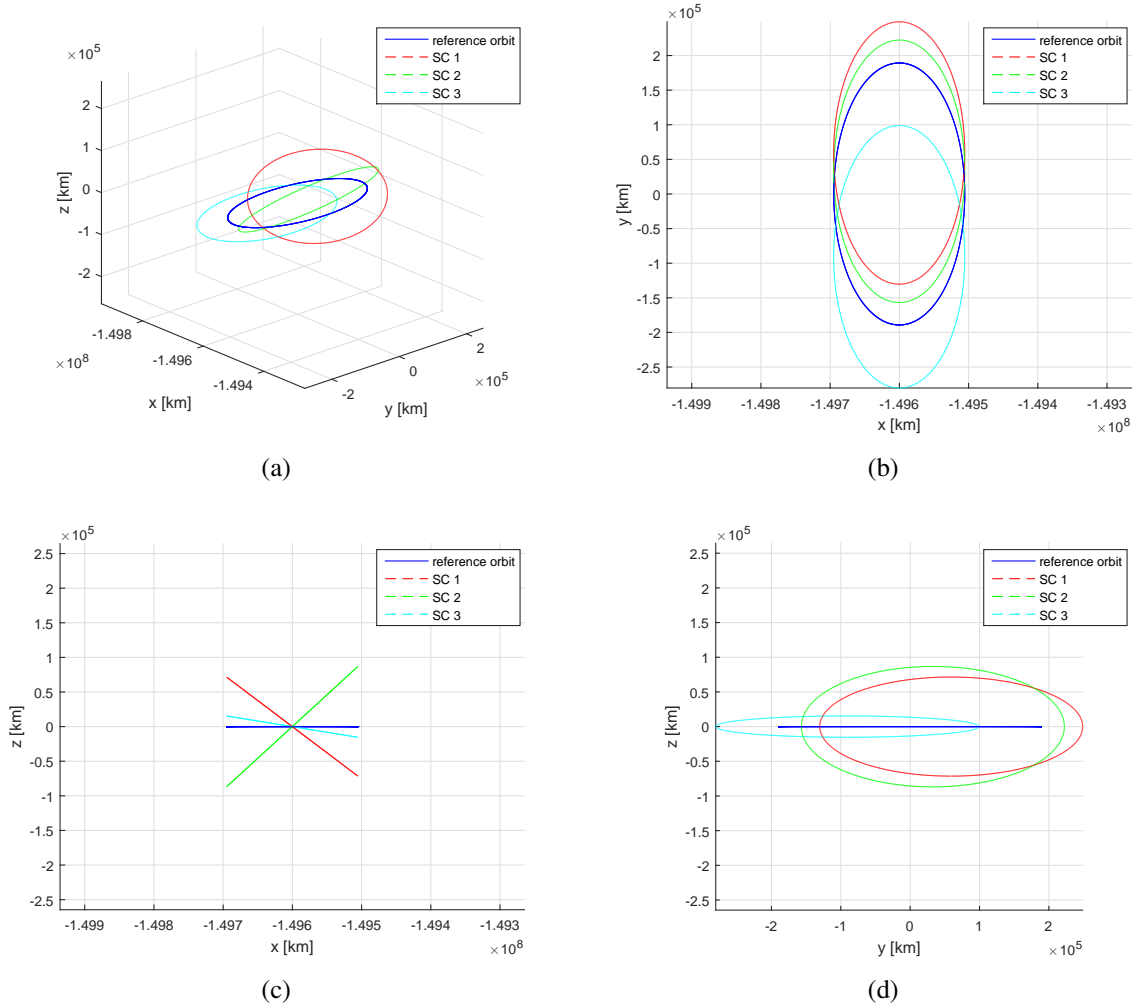


Figure 11. Orbital paths of spacecraft around reference Lyapunov orbit about L3 (a) 3D (b) x-y (c) x-z (d) y-z views

shown for the case of L1 (Fig. 5) and also with results obtained after Monte Carlo simulations [4]. The overall optimal case is indeed achieved when the n unity vector is directed towards the x axis, that is when the triangular formation lies initially on the y, z plane.

It is important to remark that only free dynamics is considered here, meaning that the formation after one orbit comes back to its initial configuration without any control action, but only through a convenient exploitation of the dynamics of the three-body system.

4.1. Comparison with ER3BP dynamics

The optimization process is repeated for the case of elliptic problem. The aim is to study whether any change occurs in the results of the optimization, under a different dynamical model. To this goal, only the best case coming out from the previous analysis is considered for comparison (orbits about L3). The optimization process is set up with only one reference orbit, which is a quasi-planar halo

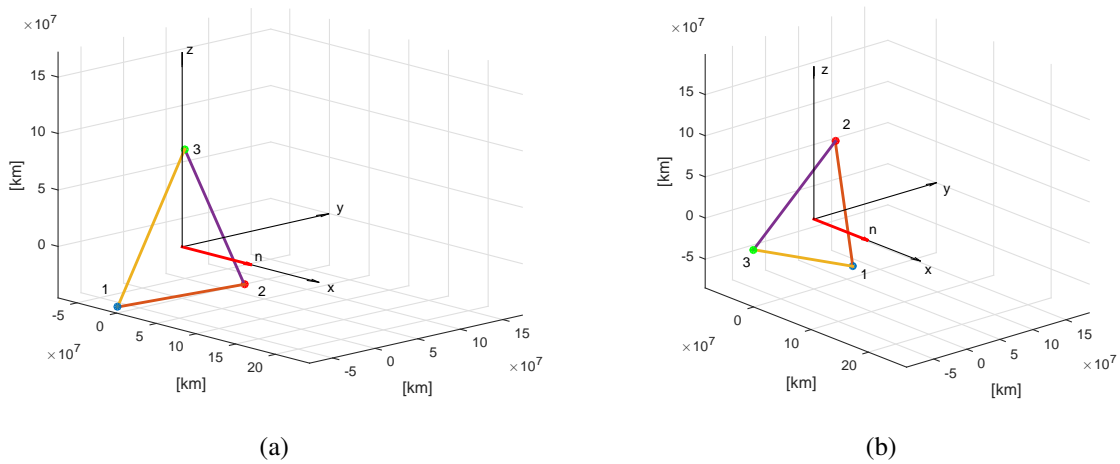


Figure 12. Optimal configuration (a) halo (b) lyapunov about L3

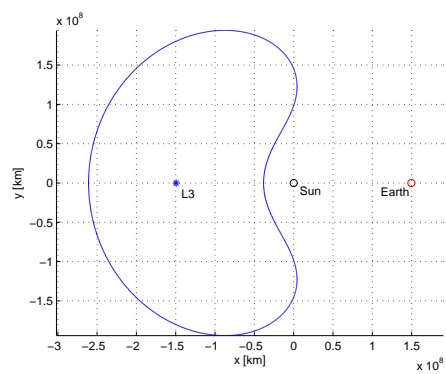


Figure 13. Quasi-planar halo orbit about L3 (Sun-Earth elliptical three-body system)

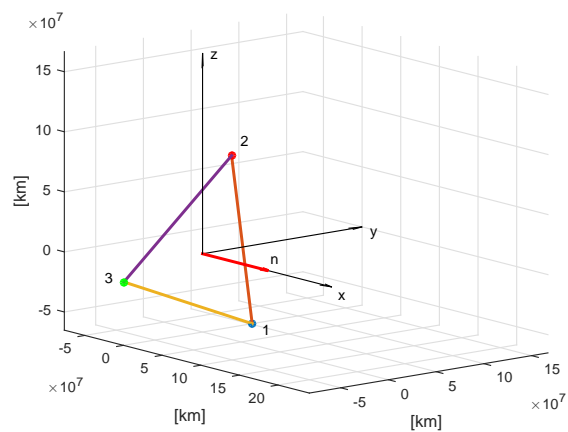


Figure 14. Optimal initial configuration for the elliptical case

orbit about L3 (Fig. 13). The latter is a resonant periodic orbit with one-year period about L3 in the elliptic Sun-Earth system.

In this case, the optimization leads to analogous results. The two performance factors after one period reach the optimal condition

$$SF = 1.00$$

$$DF = 1.00$$

and the initial orientation is found to be lying in the y - z plane (Fig. 4.1.), in agreement with previously obtained results.

5. Conclusions

The paper studies the free relative motion between three spacecraft arranged in an equilateral triangular formation, under the Circular and Elliptic Restricted Three-Body Problem formulations. An optimization process is implemented to find optimal configurations for a the three-spacecraft formation flying in the proximity of periodic orbits about collinear libration points. To evaluate the performance, a fitness function is defined to include two performance factors, which are defined to evaluate and quantify the change in shape and size of the formation during its evolution on the reference orbit. The initial population is identified with all variables needed to initiate the geometry and the dynamics of the formation. The search space of the optimizer is defined accordingly by selecting suitable boundaries for the variables in use.

As far as this study is concerned, the optimal results have been achieved for formations lying initially on the y, z plane of the synodic reference frame. This configuration is found to be optimal for difference sets of reference orbits: lyapunov and halo orbits about the three collinear libration points. Other than initial orientation, no parameters seem to play an important role on formation keeping performance. This is in agreement with previous studies on the topic [4]. It is shown that this sets of initial configurations lead to very favorable conditions in terms of formation keeping after one orbit. Moreover, the optimizer identified peculiar periodic motion in the proximity of periodic libration point orbits.

The method here proposed is useful to look for periodicity in the relative motion between the three spacecraft flying in formation. The optimization can be easily rearranged by considering a different fitness function, for example to search for suitable configurations in terms of formation keeping after half orbit or, in general, to increase the occurrence of ideal formation keeping condition during one orbital period.

6. References

- [1] Barden, B. T. and C, H. K. "Formation Flying in the Vicinity of Libration Point Orbits." AAS 98-169, 1998.
- [2] Gómez, G., Marcote, M., Masdemont, J. J., and Mondelo, J. M. "Natural Configurations and Controlled Motions Suitable for Formation Flying." AAS 05-347, 2005.

- [3] Héritier, A. and Howell, K. C. “Regions Near the Libration Points Suitable to Maintain Multiple Spacecraft.” 2012.
- [4] Ferrari, F. and Lavagna, M. “Formation Flying and Relative Dynamics Under the Circular Restricted Three-Body Problem Formulation.” *Spaceflight Mechanics 2014*, Roby S. Wilson et al. (Eds.), pp. 185–204, 2014.
- [5] Bando, M. and Ichikawa, A. “Periodic Orbits and Formation Flying Near the Libration Points.”
- [6] Ferrari, F. and Lavagna, M. “Triangular Formation Flying Under the Elliptic Restricted Three-Body Formulation.” *65th International Astronautical Congress*, 2014.
- [7] Bik, J. J. C. M., Visser, P. N. A. M., and Jenrich, O. “Stabilization of the triangular LISA satellite formation.”
- [8] Guzmán, J. J. and Edery, A. “Mission Design for the MMS Tetrahedron Formation.” *IEEEAC*.
- [9] Dow, J., Matussi, S., Mugellesi Dow, R., Schmidt, M., and Warhaut, M. “The implementation of the cluster II constellation.” *Acta Astronautica*, Vol. 54, pp. 657–669, 2004.
- [10] Szebehely, V. and Giacaglia, G. E. O. “On the Elliptic Restricted Problem of Three Bodies.” *The Astronomical Journal*, Vol. 69, No. 3, 1964.
- [11] Gurfil, P. and Meltzer, D. “Stationkeeping on Unstable Orbits: Generalization to the Elliptic Restricted Three-Body Problem.” *The Journal of the Astronautical Sciences*, Vol. 54, No. 1, 2006.
- [12] Broucke, R. “Stability of Periodic Orbits in the Elliptic, Restricted Three-Body Problem.” *AIAA Journal*, Vol. 7, No. 6, pp. 1003–1009, 1969.
- [13] Campagnola, S., Lo, M., and Newton, P. “Subregions of Motion and Elliptic Halo Orbits in the Elliptic Restricted Three-Body Problem.” *AAS 08-200*, 2008.